

LASERS

https://doi.org/10.1070/QEL16956

Pulsed laser module based on a high-power semiconductor laser for the spectral range 1500–1600 nm

Yu.K. Bobretsova, D.A. Veselov, N.V. Voronkova, S.O. Slipchenko, V.A. Strelets, M.V. Bogdanovich, P.V. Shpak, M.A. Ladugin, A.A. Marmalyuk, N.A. Pikhtin

Abstract. **A laser source for bleaching passive *Q*-switches of erbium–ytterbium lasers is developed and studied. The developed and studied compact pulsed module (peak power exceeding 10 W in a pulse with a duration of 1 μs at a wavelength around 1550 nm) is made on the basis of a semiconductor lasers with an ultra-narrow waveguide integrated with a pulsed pump card. To optimise the output laser characteristics, a series resistance was used in the laser pump circuit. The powers of the free-space and fibre-coupled modules at a temperature of 25 °C are 15 and 12 W, respectively, at a pulse shape close to rectangular.**

Keywords: *absorption coefficient, semiconductor laser, internal optical losses, pulsed pumping, energy barrier, ultra-narrow waveguide.*

1. Introduction

Lasers emitting in the spectral range 1400–1600 nm are used in various fields, including science, medicine, and telecommunications, but the most important application today is range finding [1, 2]. Distance measurement, relief scanning, and image analysis are required for rapidly developing automated ground transport aircraft and unmanned aerial vehicles. At present, the power and, hence, the effective operational range of devices are limited mainly by laser safety requirements [3]. In civil life, in particular, in unmanned aerial vehicles, the problem of eye-safe radiation is especially important. Lasers emitting in the range 1400–1600 nm are comparatively harmless because radiation with a wavelength longer than 1400 nm is absorbed in eye cornea and hence, is not focused on retina [4]. The eye-safe powers for sources of 1400–1600-nm radiation are higher than for sources emitting in the range of 800–1100 nm [3]. In addition, radiation at wavelengths exceeding 1100 nm cannot be recorded by widespread silicon detectors and arrays in principle and is weaker scattered by fine particles, which increases the operational capability of radiation under adverse weather conditions [5].

Recent advances in the study and development of high-power pulsed and cw InP-based lasers emitting near λ = 1550 nm [6, 7] made it possible to considerably increase their output optical characteristics and create a number of devices for practical applications. In the present work, we report the results on the development of a laser for bleaching a passive *Q*-switch of an erbium–ytterbium laser. Erbium–ytterbium lasers, which have a high peak power and a high spatial beam quality, are used for long-distance rangefinders. A problem of passively *Q*-switched lasers is the existence of timing jitter, which means that the time of the laser pulse start is undetermined. This problem can be solved by laser-assisted bleaching of passive *Q*-switches using a short high-power pulse of, for example, a semiconductor laser.

The aim of the present work was to develop a compact laser module for bleaching passive *Q*-switches of erbium–ytterbium lasers and for solving other scientific and industrial problems.

2. Development of requirements to the laser module

As a passive *Q*-switch of erbium–ytterbium lasers, one in most cases uses spinel doped with cobalt ions ($Co^{2+}:MgAl_2O_4$), which has some advantages compared to other materials [8–10]. The absorption band of the $Co^{2+}:MgAl_2O_4$ crystal lies mainly in the range 1300–1600 nm with a maximum at 1540–1550 nm [9]. Therefore, to bleach a saturable absorber, one should use a laser module emitting at wavelengths close to 1550 nm with the possibility of slight tuning.

Preliminary analysis of the literature and experience of working with passively *Q*-switched lasers with bleaching of saturable absorbers showed that, for efficient decrease of jitter, the bleaching pulse power density should be no lower than 25 kW cm^{-2} at a pulse duration of 1–2 μs [11], while further increase in the power density can decrease the jitter even more [12]. In addition, an increase in the bleaching pulse peak power can lead to an increase in the pulse energy of the passively *Q*-switched laser [13]. It was shown in [13] that bleaching of the passive *Q*-switch decreases the laser pulse duration and makes the pulse shape smoother due to a temporal overlap between the laser and bleaching pulses.

As a result, we chose the following desired characteristics of a laser diode for bleaching a $Co^{2+}:MgAl_2O_4$ passive *Q*-switch: maximum output power no lower than 10 W (so that the power density was 31.8 kW cm^{-2} in the case an output

Yu.K. Bobretsova, D.A. Veselov, N.V. Voronkova, S.O. Slipchenko, V.A. Strelets, N.A. Pikhtin Ioffe Institute, Russian Academy of Sciences, Politekhnicheskaya ul. 26, 194021 St. Petersburg, Russia; e-mail: nike@hpld.ioffe.ru;
M.V. Bogdanovich, P.V. Shpak B.I. Stepanov Institute of Physics, National Academy of Sciences of Belarus, prosp. Nezavisimosti 68-2, 220072 Minsk, Russia;
M.A. Ladugin OJSC 'M.F. Stelmakh Polus Research Institute', ul. Vvedenskogo 3, stroenie 1, 117342 Moscow, Russia;
A.A. Marmalyuk OJSC 'M.F. Stelmakh Polus Research Institute', ul. Vvedenskogo 3, stroenie 1, 117342 Moscow, Russia; National Research Nuclear University 'MEPhI', Kashiskoe sh. 31, 115409 Moscow, Russia

Received 30 January 2019
Kvantovaya Elektronika **49** (5) 488–492 (2019)
Translated by M.N. Basieva

fibre core diameter of 200 μm), pulse duration 1 μs, maximum pulse repetition rate 1 kHz, laser wavelength 1550 nm, aperture width 150 μm.

3. Semiconductor lasers

Lasers for the developed module were based on a double separate-confinement heterostructure with a quantum-well active region and an ultra-narrow waveguide in the AlGaInAs/InGaAsP/InP solid-solution system grown by MOCVD. The ultra-narrow heterostructure waveguide [6] makes it possible to obtain both a high efficiency in the pulsed regime and a low (about 30°) radiation divergence along the axis perpendicular to the heterostructure layers. InP emitters have profiled doping to provide low initial internal optical losses. As energy barriers, AlInAs layers are grown on the waveguide–emitter interface. Two strained quantum wells in compensating layers (with the opposite mechanical strain) are used as an active region. In general, the semiconductor laser scheme is similar to the scheme presented in [6], except for the emitter doping profile.

The lasers were fabricated using a standard shallow-mesa etching with an aperture 150 μm wide restricted by shallow-etched mesa grooves. We studied lasers with different cavity lengths and reflection coefficients of mirrors formed by natural cleavages. For the output module, we made lasers with the optimal strip waveguide length and reflection coefficients of mirrors of 5% and 95% provided by dielectric coatings. The laser crystals were mounted on copper heat sinks.

4. Pump circuit development

The problem of pumping lasers by short ($\sim$100 ns) current pulses is related to a low series resistance of semiconductor diodes R_s (typical value is about 50 mΩ) and to high amplitudes of required current pulses. In this operation regime, the main factor limiting the device characteristics is the inductance in the laser pump circuit. This inductance is caused by the parasitic inductance of the laser, transistors, contact plates and paths, conductors connecting the laser with the pump card, and other elements of the circuit. The inductance limits not only the minimum current pulse duration, but also the maximum current amplitude. After the pulse termination, the magnetic field energy stored for the pulse time forms a reverse voltage overshoot, which may break the laser diode, while the use of a fast back-to-back diode for protection is not always effective.

There exist two methods for solving the inductance problem. The first way is to suppress the parasitic inductance by decreasing the length of all conductors and placing the laser most closely to the elements forming the current pulse. The second method consists in the use of a series load resistance R in the pump circuit. An increase in the nominal value of this resistance makes it possible to increase the operation speed of the pump circuit, but this simultaneously decreases the scheme efficiency and increases the needed power supply voltage.

At a pulse duration of 1 μs, there are no special requirements to the durations of the leading and trailing fronts, but steep edges and a regular shape of pulses are important for obtaining both high electric pumping efficiency and high optical pulse energy. In the present work, we use both methods for inductance suppression; in particular, the pump card is designed so that the semiconductor laser was placed tightly to the main pump elements, i.e., capacitors and transistors. Resistance R formed of several parallel SDM resistors can be included into the pump circuit in series with the laser. The pump current pulse in the developed electric circuit is formed by four parallel fast silicon transistors. Energy for the pulse is supplied by two ceramic capacitor banks. The scheme uses two fast protective diodes. Such paralleling is used to decrease the parasitic inductance. The pump current amplitude is controlled without current feedback by changing the control voltage, which is the main power supply voltage. The pump circuit operates with a supply voltage varying from 0 to 30 V, an auxiliary voltage of 12 V, and a triggering pule with an amplitude of 5 V.

The pump card is placed inside a standard HHL-type housing with a Peltier element, a thermistor, and the laser (Fig. 1). The Peltier element, which removes heat to the lower side of the housing, has a good thermal contact not only with the laser but also with the card, thus providing cooling of its elements. The Peltier element together with the thermistor stabilise the laser temperature. The housing dimensions are $45 \times 30 \times 20$ mm without allowance for contacts.

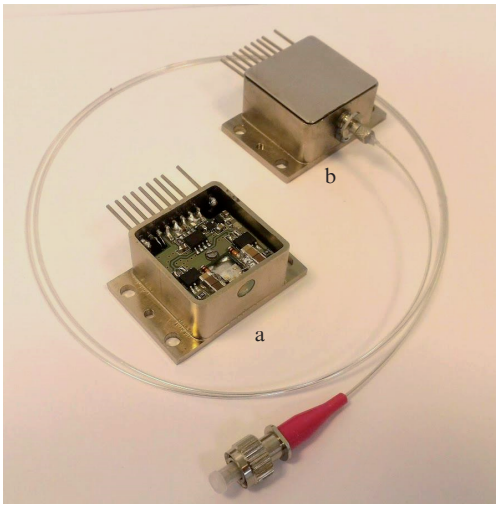

Figure 1. Developed (a) free-space and (b) fibre-coupled laser modules.

We developed and fabricated two modules (Fig. 1), with a free-space output through a window and with a fibre-coupled output. The fibre had a core diameter of 200 μm and a numerical aperture of 0.22. Below, we will mainly present the results for the free-space module. The fibre-coupled module characteristics completely coincide with the characteristics of the free-space module taking into account the injection coefficient, which is 80%–85%.

5. Study of the laser module

Semiconductor lasers operating with a low pulse repetition rate were studied in a number of works, but the pulse duration in most cases either was 10–300 ns [6, 14–16] or exceeded 10 μs [16, 17]. The first of the mentioned regimes is purely pulsed, at which self-heating of the laser almost does not affect its characteristics. The second regime corresponds to quasi-cw operation, at which the laser is rather strongly heated for the pulse duration, because of which the optical pulse shape becomes strongly distorted and the power in the middle of

the pulse becomes lower than the peak power. Thus, the pulse duration of 1 μs corresponds to an intermediate laser operation regime, which is almost unstudied at present.

The main aim of the study was not only to describe the laser characteristics in this operation regime but also to determine the optimal nominal of series resistance R, which is related to the parasitic inductance of the circuit and, hence, cannot be calculated in advance.

For different values of resistance R beginning from zero, i.e., from short circuit, we measured the dependences of the optical power on the supply voltage and recorded photoresponces (oscillograms of optical pulses). The measurements were performed by a standard method [18]. The frequency bands of the used oscilloscope (200 MHz) and photodetector (100 MHz) allow high-resolution recording of fronts with a minimum duration of 5 ns.

The dependences of the optical peak power on the supply voltage are shown in Fig. 2a. It is obvious that the maximum current and, therefore, the laser power increase with decreasing resistance R. One can see from Fig. 2 that, at short circuit ($R = 0$), the maximum power of 18.6 W is achieved at a supply voltage of only 7 V. With increasing resistance, it is necessary to use a higher supply voltage, but, on the other hand, requirements to the accuracy of its application decrease. The dependences shown in Fig. 2a can be transformed into traditional light–current characteristics (LCCs) by measuring the pulsed current flowing through the laser, for example, by measuring the series resistor voltage. In our case, the module design did not allow us to perform these measurements, because of which we determined the LCC by another method. Since the LCC and the current–voltage characteristic (CVC) of the laser are independent of the external pump circuit, all dependences shown in Fig. 2a should lie on one curve when plotted as functions of current.

In this connection, pump current I can be approximately represented in the form

$$I = (U - U_0)/(R + R_s), \quad (1)$$

where U is the supply voltage, U_0 is the cutoff voltage, and R is the resistance connected to the laser. In the given case, R_s is related not only to the laser but also to the resistance of the rest scheme (transistors, capacitors, and conductors).

We chose U_0 and R_s so that all LCCs were reduced to one curve; the currents for all curves in this case were calculated from (1). The obtained LCCs are shown in Fig. 2b, and the obtained parameters for the laser CVC were $U_0 = 1.5$ V and $R_s = 65$ mΩ. Despite the approximate character of these values, they can be used for calculations of pump circuits.

In the case of short circuit, when current cannot be directly measured in principle, this analysis allowed us to estimate the maximum current to be 80–90 A at a supply voltage of 7 V. Further increase in the supply voltage is obviously useless due to the LCC saturation.

Based on Figs 2a and 2b, we can suggest that the best solution is the absence of resistor R in the pump circuit. However, study of the laser photoresponses showed that the optical pulse shape in this case is strongly distorted. While the pulse shape at a high series resistance R (1.5 Ω and higher) is rectangular with short fronts (15–20 ns), the peak power in the case of short circuit ($R = 0$) is observed in the beginning of the pulse and considerably decreases to the pulse end, while the leading front in this case expands to about 100 ns. Table 1 lists the leading front durations and the intensity decay during the pulse for different resistances R and supplying voltages. The oscillograms of optical pulses for resistance $R = 0.45$ Ω are presented in Fig. 3.

The data in Table 1 show that a decrease in resistance R leads to an increase in the leading front duration and to a decrease in the ratio of intensities at the pulse end and at the peak, i.e., to distortion of the pulse shape. With increasing

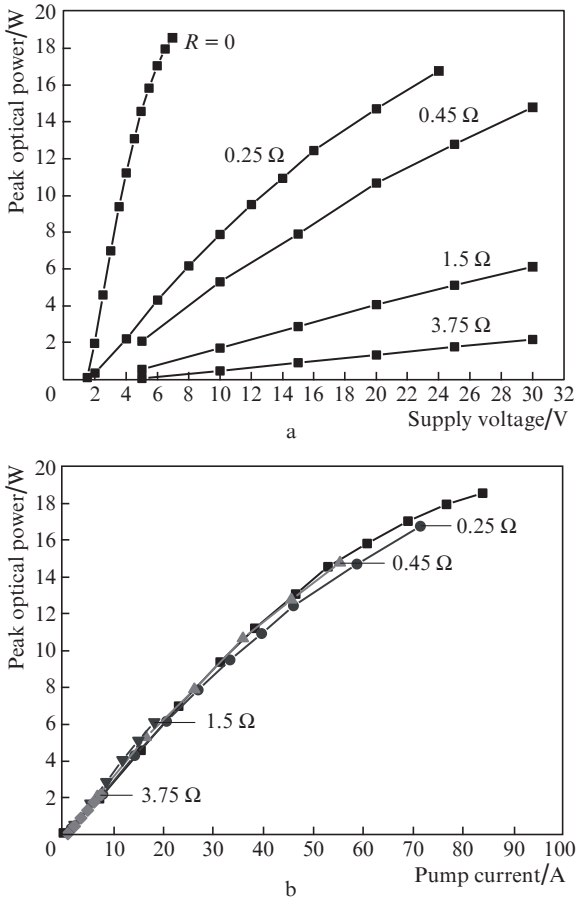

Figure 2. Peak optical powers of the pulsed laser for different resistances R versus (a) supply voltage and (b) current calculated at $U_0 = 1.5$ V and $R_s = 65$ mΩ. Temperature 25°C, pulse repetition rate 1 kHz, free-space output.

Table 1. Parameters of optical pulses at different nominal resistances R connected in series with the laser and different supply voltages.

Resistance/Ω	Supply voltage/V	Leading front duration at a level of 10%–90%/ns	Ratio of the amplitude at the pulse end to the peak amplitude (%)
3.75	30	15	100
1.5	30	19	100
0.45	10	21	100
0.45	20	22	97
0.45	30	25	91
0.25	16	28	96
0.25	20	27	90
0.25	24	24	86
0	5	109	78
0	6	91	73
0	7	80	70

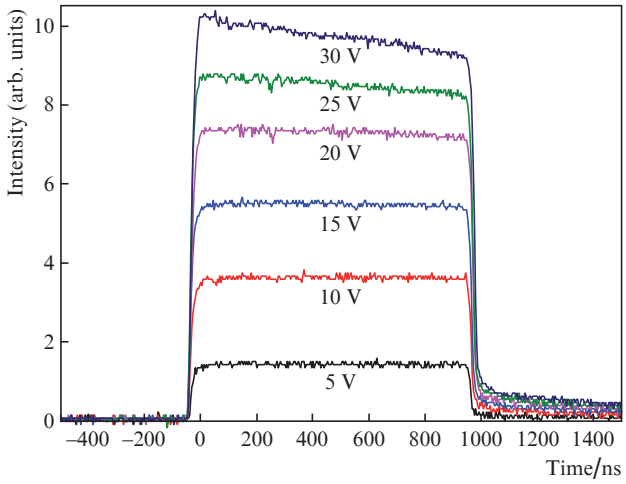

Figure 3. Oscillograms of optical pulses of the laser module at different (5–30 V) supply voltages. Temperature 25°C, $R = 0.45$ Ω, pulse repetition rate 1 kHz, free-space output.

supply voltage, the front duration either almost does not change or decreases, while the signal shape is gradually distorted.

The leading front shape in this case is related to the parasite inductance suppression efficiency. At a high resistance R, when inductance only slightly affects the operation speed, the front durations are determined by the operation speed of switches (field-effect transistors). As seen from Table 1, the leading front duration, which is determined by field-effect transistors, is 15–20 ns.

The pulse shape depends on two main factors, namely, on laser self-heating during the current pulse and on the capacitor bank discharge. The first factor makes is possible to explain the gradual change in the pulse shape with increasing pump current. According to Fig. 3 and Table 1, the optical pulse shape remains rectangular up to a supply voltage of 20 V. With farther increase in in the pump current, one observes a noticeable distortion of the pulse shape, while the capacitor bank capacitance decreases with increasing voltage by less than 10%. This testifies to a decrease in the lasing efficiency during the current pulse.

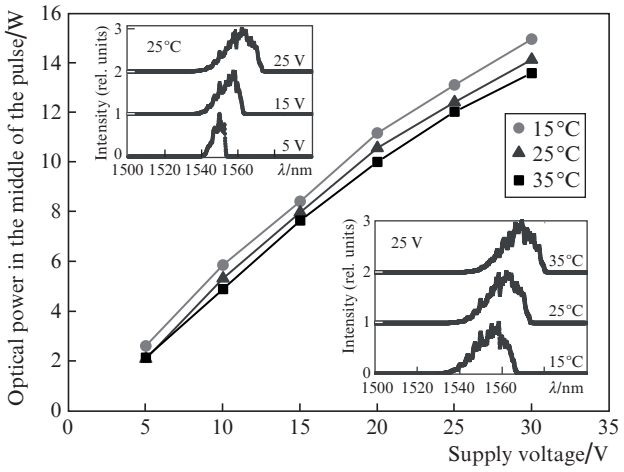

Figure 4. Dependences of the laser power and spectra (insets) on the supply voltage (5, 15, and 25 V) and laser temperature (15, 25, and 35°C). Pulse repetition rate 1 kHz, free-space output.

As resistance R decreases, the pump circuit time constant decreases, which leads to distortion of the shape of the current pulse and, hence, of the optical pulse, which can be seen in Table 1 for $R = 0$ and 0.25 Ω. From the obtained data, we chose the optimal resistance equal to 0.45 Ω.

Figure 4 shows the dependences of the laser module optical power on the pump current at different temperatures and supply voltages for a pulse repetition rate of 1 kHz. The optical powers presented in Fig. 4 were measured in the middle of the optical pulse at the exit from the laser module window. Figure 4 also shows the corresponding laser spectra. One can see that it is possible to control the laser spectrum position by keeping a particular temperature and simultaneously to maintain a constant optical power by tuning the supply voltage.

The maximum achieved pulsed optical power was 15 W, while the possibility of controlling the laser spectrum (with a constant power) existed at optical powers up to 13 W. The maximum output power for the fibre-coupled laser was about 12 W.

Figure 5 presents the angular dependences of radiation intensity at the exit from the laser module window along two directions, namely, parallel and perpendicular to the heterostructure layers. As was expected, the FWHM divergence angle in the perpendicular direction is 31° and almost does not depend on the pump current amplitude. The divergence along the parallel axis is determined by the multimode strip waveguide 150 μm wide and increases from 8.5 to 15° with increasing pump current amplitude. As a whole, such dependences are typical for multimode semiconductor lasers. To collimate this radiation, it is better to use aspherical lenses with numerical apertures of 0.5–0.6.

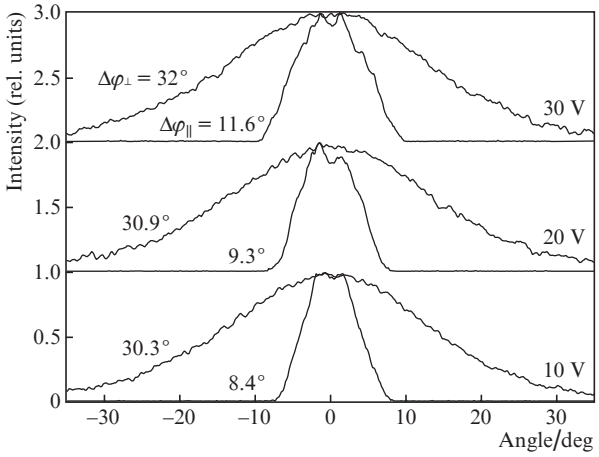

Figure 5. Angular dependences of far-field laser intensity (FWHM) along the axes parallel (∥) and perpendicular (⊥) to the heterostructure layers for supply voltages of 10, 20, and 30 V. Temperature 25°C, pulse repetition rate 1 kHz, free-space output.

The radiation divergence of the fibre-coupled laser module corresponds to the divergence of a multimode fibre with a numerical aperture of 0.22.

6. Conclusions

We have fabricated, studied, and optimised laser modules emitting in the spectral range 1500–1600 nm for bleaching passive Q-switches of erbium–ytterbium lasers. The modules

consist of lasers based on double separate-confinement heterostructure with an ultra-narrow waveguide and quantum wells in the active region. A pulsed pump source is developed, which is built into a standard HHL-type housing and integrated with a laser diode. Optical pulses with power of 15 W, duration of 1 μs, repetition rate up to 1 kHz, and a shape close to rectangular are obtained. It is found that, for the given laser, pump circuit card, and operation regime, the connection of resistors with a total nominal resistance of 0.45 Ω in series with the laser makes it possible to achieve the optimal combination of the signal shape and power. The laser modules can have free-space or fibre-coupled outputs and provide the possibility of controlling the laser power and temperature.

Acknowledgements. This work was supported by the Russian Foundation for Basic Research (Grant No. 18-52-00022).

References

1. Steinvall O., Persson R., Berglund F., Gustafsson O.K.S., Gustafsson F. *Proc. SPIE*, **9080**, 90800W (2014).
2. Hecht J. *Opt. Photonics News*, **29** (1), 26 (2018).
3. Safety of Laser Products – Part 1: Equipment Classification and Requirements, document IEC 60825-1:2014, International Electrotechnical Commission (2014).
4. Bloom S., Korevaar E., Schuster J., Willebrand H. *J. Opt. Net.*, **2** (6), 178 (2003).
5. Samman A., Rimai L., McBride J.R., Carter R.O., Weber W.H., in *Proc. 52nd Veh. Technol. Conf.* (VTC) (Boston, USA, 2000) pp 2084–2089.
6. Marmalyuk A.A., Ryaboshtan Yu.L., Gorlachuk P.V., Ladugin M.A., Padalitsa A.A., Slipchenko S.O., Lyutetskii A.V., Veselov D.A., Pikhtin N.A. *Quantum Electron.*, **47** (3), 272 (2017) [*Kvantovaya Elektron.*, **47** (3), 272 (2017)].
7. Marmalyuk A.A., Ryaboshtan Yu.L., Gorlachuk P.V., Ladugin M.A., Padalitsa A.A., Slipchenko S.O., Lyutetskii A.V., Veselov D.A., Pikhtin N.A. *Quantum Electron.*, **48** (3), 197 (2018) [*Kvantovaya Elektron.*, **48** (3), 197 (2018)].
8. Karlsson G., Pasiskevicius V., Laurell F., Tellefsen J.A., Denker B., Galagan B., Osiko V., Sverchkov S. *OSA TOPS*, **50**, 72 (2001).
9. Mikhailov V.P., Yumashev K.V., Denisov I.A., Prokoshin P.V., Posnov N.N., Moncorge R., Vivien D., Ferrand E., Guyot Y. *OSA TOPS*, **26**, 317 (1999).
10. Mlynczak J., Belghachem N., Kopczynski K., Kisielewski J., Stepien R., Wychowaniec M., Galas J., Litwin D., Czyzewski A. *Opt. Quant. Electron.*, **48** (247), 1 (2016).
11. Cole B., Lei J., DiLazaro T., Schilling B., Goldberg L. *OSA Appl. Opt.*, **48** (31), 6008 (2009).
12. Bogdanovich M.V., Grigor'ev A.V., Kot A.N., Lantsov K.I., Lepchenkov K.V., Ryabtsev A.G., Ryabtsev G.I., Shpak P.V., Shchemelev M.A., Veselov D.A., Pikhtin N.A. *Progrmma i tezisy dokladov Rossiiskogo simposiuma s mezhdunarodnym uchastiem "Poluprovodnikovye lasery: fizika i tekhnologiya"* (Programme and proceedings of the 6th Russian symposium with international participation. "Semiconductor Lasers: Physics and Technology") (St. Petersburg, 2018).
13. Zhang B., Chen Y., Wang P.Y., Wang Y., Liu J., Hu S., Xia X., Sang Y., Yuan H., Cai X., Liu D., Gai B., Guo J. *OSA Appl. Opt.*, **57** (16), 4595 (2018).
14. Veselov D.A., Pikhtin N.A., Lyutetskii A.V., Nikolaev D.N., Slipchenko S.O., Sokolova Z.N., Shamakhov V.V., Shashkin I.S., Kapitonov V.A., Tarasov I.S. *Quantum Electron.*, **45** (7), 597 (2015) [*Kvantovaya Elektron.*, **45** (7), 597 (2015)].
15. Knigge A., Klehr A., Wenzel H., Zeghuzi A., Fricke J., Maaßdorf A., Liero A., Tränkle G. *Phys. Stat. Sol.*, **215** (8), 1700439 (2018).
16. Wang X., Crump P., Pietrzak A., Schultz C., Klehr A., Hoffmann T., Liero A., Ginolas A., Einfeldt S., Bugge F., Erbert G., Tränkle G. *Proc. SPIE*, **7198**, 71981 G (2009).
17. Ladugin M.A., Marmalyuk A.A., Padalitsa A.A., Bagaev T.A., Andreev A.Yu., Telegin K.Yu., Lobintsov A.V., Davydova E.I., Sapozhnikov S.M., Danilov A.I., Podkopaev A.V., Ivanova E.B., Simakov V.A. *Quantum Electron.*, **47** (4), 291 (2017) [*Kvantovaya Elektron.*, **47** (4), 291 (2017)].
18. Veselov D.A., Kapitonov V.A., Pikhtin N.A., Lyutetskii A.V., Nikolaev D.N., Slipchenko S.O., Sokolova Z.N., Shamakhov V.V., Shashkin I.S., Tarasov I.S. *Quantum Electron.*, **44** (11), 993 (2014) [*Kvantovaya Elektron.*, **44** (11), 993 (2014)].